JOURNAL OF SOLID STATE CHEMISTRY **23**, 11–18 (1978)

Order–Disorder Transition of the Metal Vacancies in the Vanadium–Sulfur System. I. An Experimental Study

Y. OKA, K. KOSUGE, AND S. KACHI
Department of Chemistry, Faculty of Science, Kyoto University, Kyoto, Japan

Received March 30, 1977; in revised form May 24, 1977

The phase diagram of the VS–VS_2 system was studied by high-temperature DTA and X-ray measurements. As a result, it has been confirmed that the vacancy-ordered V_3S_4-type structure transforms into the CdI_2-type structure at T_{c1}, while the vacancy-ordered V_5S_8-type structure shows successive transformations on heating; V_5S_8 type $\xrightarrow{T_{c2}}$ V_3S_4 type $\xrightarrow{T_{c1}}$ CdI_2 type. The mechanisms of the phase transitions are discussed from the viewpoint of structural relationships. The phase diagram of the VS–VS_2 system is constructed in the temperature range up to 1200°C. In the V–Se system similar results to those in the V–S system have been obtained. The V–S–Se system has also been studied and the result supports the above-mentioned results on the V–S and V–Se systems.

1. Introduction

The 3*d* transition metal chalcogenides M–X, where M = Ti, V, Cr and X = S, Se, Te, have the NiAs-type or the related NiAs-type structure at the composition of MX and the CdI_2-type structure at MX_2. Between these extreme structures, there appear many phases originating from ordering of metal vacancies. These vacancies are located in the alternate metal layers along the *c* axis. A stacking of metal layers can be regarded as alternate arrays of fully occupied and partially occupied layers. At low concentrations of vacancies (δ_1 in $M_{1-\delta_1}X$) the nonstoichiometric NiAs phase is stabilized because the interaction energy between vacancies is small (random distribution). With increase of δ_1, the interaction energy between vacancies causes ordering of the vacancies and many types of the vacancy-ordered phase appear. When the vacancy concentration δ_1 becomes close to $\frac{1}{2}$, the nonstoichiometric CdI_2 phase (random distribution) is stabilized.

Possible ordered structures can be constructed by supposing the metal concentration (δ_2 in $M_{1+\delta_2}X_2$) of a partially occupied layer as follows; M_7X_8 with $\delta_2 = \frac{3}{4}$, M_5X_6 with $\delta_2 = \frac{2}{3}$, M_3X_4 with $\delta_2 = \frac{1}{2}$, M_2X_3 with $\delta_2 = \frac{1}{3}$, and M_5X_8 with $\delta_2 = \frac{1}{4}$.

For the Ti–S system, Wiegers and Jellinek (*1*) proposed the concept of occupation waves along the *c* axis in order to interpret the intensities of Debye–Scherrer diffraction peaks of many phases. In the V–S system, it has been confirmed that there are only two vacancy-ordered phases with the $M_{1+\delta_2}X_2$ stoichiometry, V_3S_4 and V_5S_8 (*2*, *3*). In the Cr–S system many phases such as Cr_7S_8, Cr_5S_6, Cr_3S_4, and Cr_2S_3 were found to exist between CrS and $CrS_{1.50}$ (*4*). Thus these metal–sulfur systems show different modes of vacancy-ordered phase formation.

Here we restrict ourselves to the problems of phase transition by vacancy order–disorder. The phase transition must be observed by changing the composition, i.e., vacancy concentration as mentioned above, or by increasing the temperature at a fixed composition. By increasing the temperature, the low-temperature ordered phase gradually loses the degree of order and at the critical temperature T_c transforms to the high-temperature ordered or disordered phase. For the NiAs based struc-

0022-4596/78/2312-0011 $02.00/0
Copyright © 1978 by Academic Press, Inc.
All rights of reproduction in any form reserved.
Printed in Great Britain

ture, the process of disordering may be as follows. The ordered structure → the intralayer rearrangement (ordered phase) → the intralayer disorder (nonstoichiometric CdI_2 type) → the interlayer disorder (nonstoichiometric NiAs type).

To our knowledge, few reports have been published on this theme (*5*). The V–S system is quite suitable because it has only two types of ordered structures within a wide nonstoichiometric composition range (*2*). But in this system, the crystal structure of the sample, obtained by rapid quenching from high temperature, is always the low-temperature ordered structure, so the high-temperature crystal structure must be determined *in situ*. Previously, Nakazawa *et al.* (*6*) carried out high-temperature X-ray measurements on a V_5S_8 single crystal. They found that the intralayer order–disorder transition occurs at around 800°C.

In the present work the phase diagram of the V–S system in the composition range from $VS_{1.30}$ to $VS_{1.70}$ has been determined in detail by high-temperature DTA and X-ray methods. And, complementarily, the V–S–Se system was also studied, and the result of the study supports those of the V–S and V–Se system.

2. Experimental Details

The samples were synthesized by the direct reaction from the elements. For the V–S system, vanadium powder (99.9%) and sulfur powder (99.999%) were sealed in an evacuated silica tube, heated at 800°C for 2 weeks, and quenched in water. For the V–Se system, vanadium powder and granular selenium (99.999%) were used for starting materials. For the V–S–Se system, vanadium powder, sulfur powder, and granular selenium were used. The phase of the sample was determined by the X-ray method and the composition was analyzed by oxidizing the sample in air to V_2O_5.

The high-temperature DTA measurement was carried out by Rigaku Thermoflex DTA. A micro silica capsule sealed in vacuum was used to contain the sample. Al_2O_3 was used as a reference. The measured temperature range was from room temperature to 1200°C.

The high-temperature X-ray measurements were carried out by the film method using a Shimadzu high-temperature X-ray camera and by the counting method using a Rigaku high-temperature attachment. In both methods, the sample was sealed in vacuum in a silica capillary with a very thin wall about 0.01 mm thick. The maximum temperature was 1100°C for the film method and 1000°C for the counting method.

3. Result and Discussion

3.1. Phase Identification at Room Temperature

The quenched samples were identified at room temperature by X-ray powder diffraction ($CuK\alpha$). As will be shown later, it is impossible to quench the high-temperature phase. It is known (*2*) that there exist two phases, V_3S_4 and V_5S_8, between VS and VS_2. The V_3S_4 phase exists in the composition range from $VS_{1.18}$ to $VS_{1.56}$ and the V_5S_8 phase from $VS_{1.57}$ to $VS_{1.68}$. By the above-mentioned method, it has not been possible to prepare samples with sulfur content greater than $VS_{1.64}$. With increasing sulfur content, the V_3S_4-type crystal structure transforms into the V_5S_8 type at about $VS_{1.56}$, i.e., no two phase region was observed within experimental error.

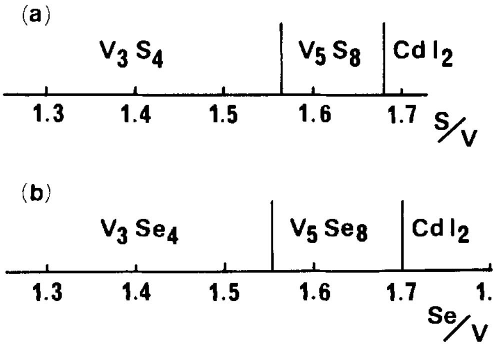

FIG. 1. Phase relation at room temperature. Samples were obtained by rapid quenching from 800°C. The two phase region was hardly observed. (a) V–S system. (b) V–Se system.

This suggests that the transformation from V_3S_4- to V_5S_8-type crystal structure may be of second order. For the case of the V–Se system, the phase boundary and the feature of the phase transition ($V_3Se_4 \rightarrow V_5Se_8$) are similar to the case of the V–S system. The results are summarized in Fig. 1.

3.2. DTA Measurement

The DTA curves obtained in the V–S system show the characteristic features of each phase (Fig. 2). For the samples with the V_3S_4 structure at low temperature, the curve has only one endothermic peak at T_{c_1} in the measured temperature range. The peak for the stoichiometric V_3S_4 ($VS_{1.33}$) is rather sharp; with increasing sulfur content the peak grows gradually broader. The T_{c_1} decreases with increasing sulfur content as shown in Fig. 2. On the other hand, for the samples with the V_5S_8 structure at low temperature, the DTA curve shows two endothermic peaks; the higher one is at T_{c_1} and the lower one is at T_{c_2}.

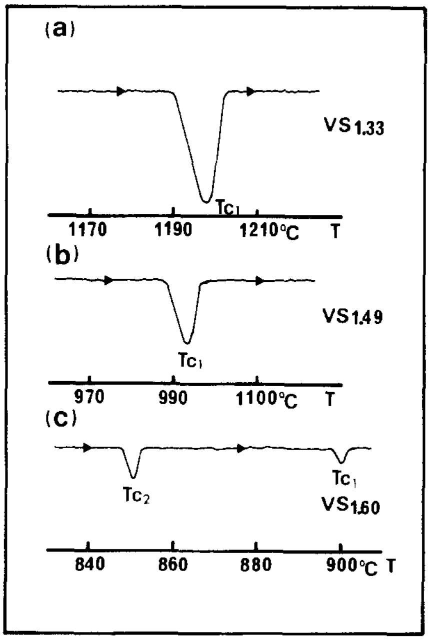

FIG. 2. DTA curves for the V–S system. (a) $VS_{1.33}$ (V_3S_4 phase); (b) $VS_{1.49}$ (V_3S_4 phase); (c) $VS_{1.60}$ (V_5S_8 phase).

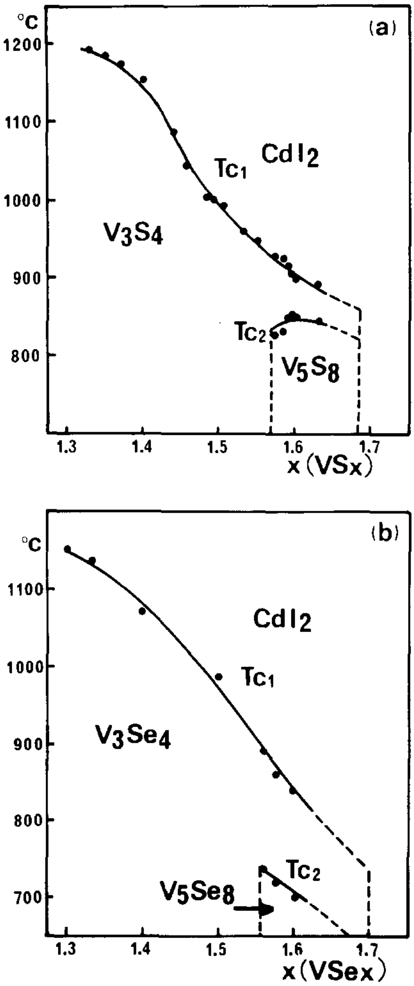

FIG. 3. Phase diagram determined by the DTA and the high-temperature X-ray measurements. The dotted lines are the speculated phase boundaries. (a) V–S system. (b) V–Se system.

The T_{c_1} in the V_3S_4 samples is smoothly connected to the T_{c_1} in the V_5S_8 samples. The peak at T_{c_2} is quite characteristic of the V_5S_8 phase. The T_{c_2} gradually decreases with increasing sulfur content. The composition dependence of T_{c_2} is not so remarkable. The phase transition at T_{c_2} seems to be of second order. The result is shown in Fig. 3a.

In the V–Se system, the DTA measurement shows behavior quite similar to that of the V–S system. The phase transition temperatures T_{c_1} and T_{c_2} are somewhat lower than those of the V–S system, as shown in Fig. 3b.

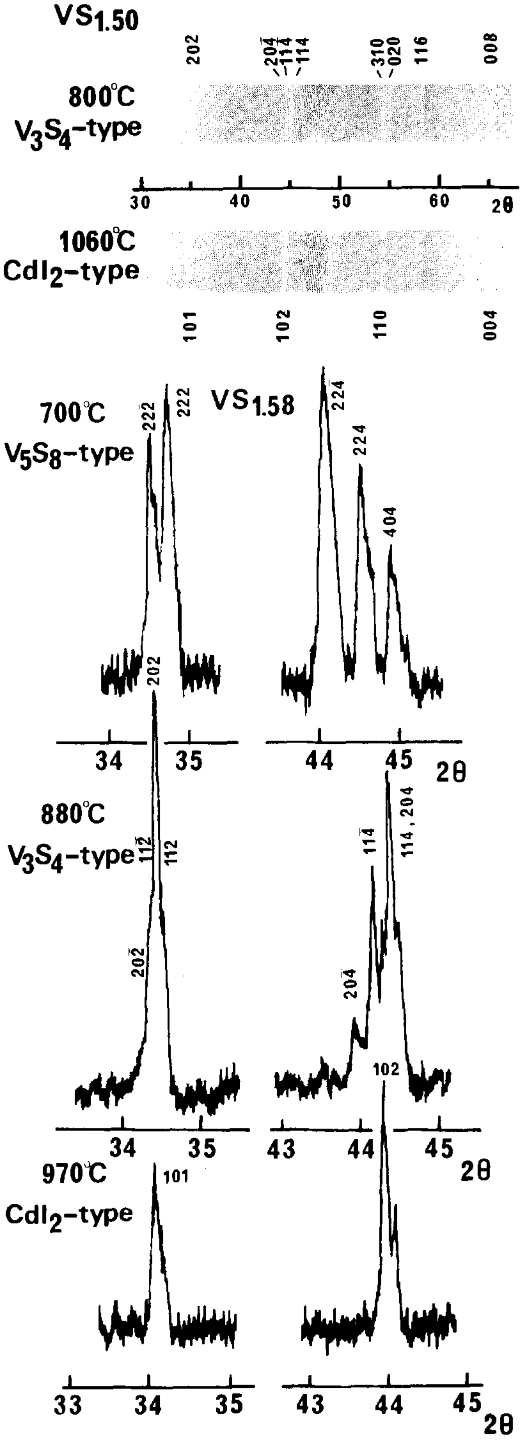

FIG. 4. High-temperature X-ray diffraction patterns. (a) The powder patterns by the film method taken at 800 and 1060°C for $VS_{1.50}$ (V_3S_4 phase at room temperature). (b) The powder patterns by the counting method taken at 700, 880, and 970°C for $VS_{1.58}$ (V_5S_8 phase at room temperature).

3.3. High-Temperature X-ray Measurement

In order to clarify the phase transitions at T_{c_1} and T_{c_2}, high-temperature X-ray measurements were carried out at temperatures up to 1100°C. The X-ray powder patterns were obtained by the film or counting method.

For example, we show here the temperature dependence of the diffraction patterns for the samples of $VS_{1.50}$ and $VS_{1.58}$ which have the V_3S_4- and the V_5S_8-type structure at room temperature, respectively. As mentioned above, T_{c_1} for $VS_{1.50}$ is about 1000°C. Figure 4a shows the typical diffraction patterns for $VS_{1.50}$ taken at 800 and 1060°C. The result shows clearly the structural transformation from the V_3S_4- to the CdI_2-type structure at T_{c_1}. As shown in Fig. 4b, the sample $VS_{1.58}$, which has transition temperatures at 920°C (T_{c_1}) and 840°C (T_{c_2}), shows the successive transformation of the crystal structure, i.e., V_5S_8 type → V_3S_4 type → CdI_2 type.

Thus, it has been clarified that the V_5S_8-type structure transforms into the V_3S_4-type for the first step and then into the CdI_2-type structure. The mechanism of the phase transition will be discussed in Section 3.5.

For the V–Se system, the result is very similar to that of the V–S sysem, as shown in Fig. 3b.

3.4. The V–S–Se System

As mentioned above, the phase diagram of the V–Se system is similar to that of the V–S system. An attempt was made to determine the phase diagram of the ternary system V–S–Se. In this section, we discuss only two points of the results which seem to be important for the understanding of the mechanism of the phase transitions.

Figure 5 shows the phase relation of the pseudobinary $VS_{1.60}$–$VSe_{1.60}$ or $V_5(S_{1-x}Se_x)_8$ system, and also the x dependence of the lattice parameter of the c axis (perpendicular to the metal layer) and the monoclinic angle β.

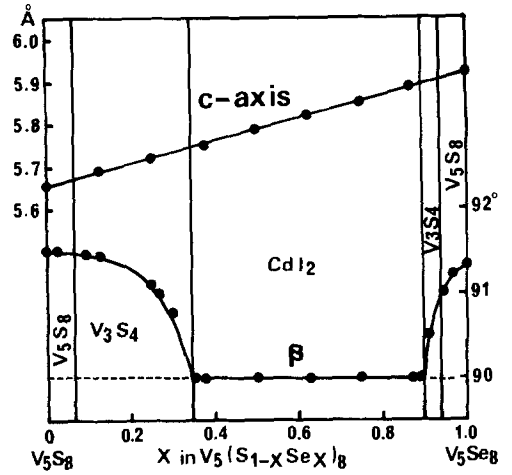

FIG. 5. Phase relation of the $V_5(S_{1-x}Se_x)_8$ system obtained at room temperature.

Although we had expected the formation of a solid solution between V_5S_8 and V_5Se_8, the result obtained is quite different. With increasing x, the phase transition takes place successively as

V_5S_8 type $(0 \leq x < 0.06)$ V_3S_4 type $(0.06 < x < 0.35)$ → CdI_2 type $(0.35 < x < 0.90)$ → V_3S_4 type $(0.90 < x < 0.94)$ → V_5S_8 type $(0.94 < x \leq 1.00)$.

This peculiar result can be interpreted as the result of x dependence of T_{c_1} and T_{c_2}, as shown schematically in Fig. 6. The phase transition temperatures T_{c_1} and T_{c_2} decrease rapidly for x less than about 0.5, and increase for larger x values. At room temperature the state of section AA' is obtained.

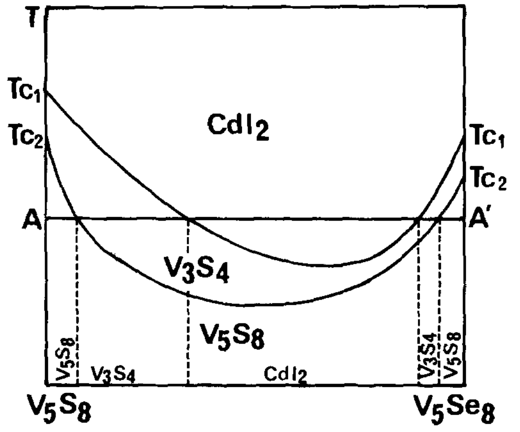

FIG. 6. Supposed phase diagram for the $V_5(S_{1-x}Se_x)_8$ system. The line AA' is the section which shows the phase relation obtained experimentally in Fig. 5 (see text).

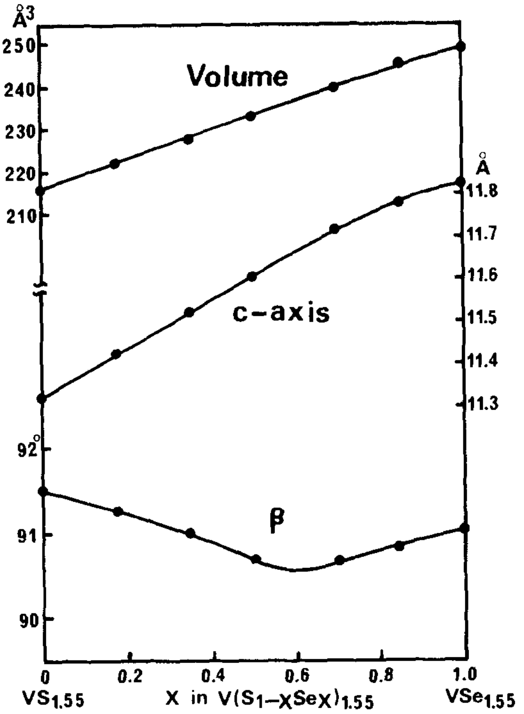

FIG. 7. Lattice parameters vs composition curves of the $V(S_{1-x}Se_x)_{1.55}$ system. β is the monoclinic angle.

In Fig. 7, the lattice parameters and unit-cell volume of $VS_{1.55}$–$VSe_{1.55}$ (or $V(S_{1-x}Se_x)_{1.55}$) are shown. Each of the end compositions ($VS_{1.55}$ and $VSe_{1.55}$) is located near the phase boundary between the V_3S_4 and V_5S_8 phases. In this system, the V_3S_4 structure type appears in the whole range of composition. However, it is to be noted that the monoclinic angle β, which shows the degree of inclination of the c axis to the metal layer due to ordering, tends to become 90° (the value of the CdI_2 type) in the intermediate region of this system.

3.5. The Mechanism of the Phase Transition

A possible mechanism of the phase transitions, i.e., $V_5S_8 \rightarrow V_3S_4 \rightarrow CdI_2 \rightarrow NiAs$, is

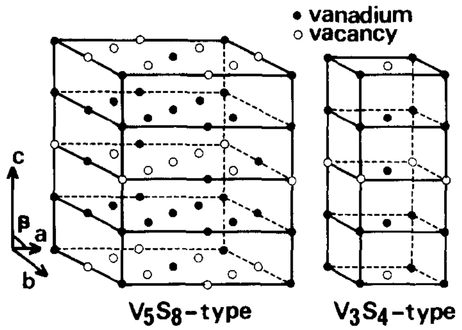

FIG. 8. Schematic illustration of the crystal structures of the V_5S_8 type and the V_3S_4 type. Only metal sites are shown. Filled circles indicate the vanadium atoms and open circles indicate the vacancy sites.

discussed in detail from the viewpoint of the structural relationships.

The crystal structures of V_3S_4 and V_5S_8 were determined by Chevreton and Sapet (*7*) and Brunie and Chevreton (*8*), and, recently, Kawada *et al.* (*9*) in detail. The crystal structures of V_3S_4 and V_5S_8 are depicted in Fig. 8.

For simplicity we discuss the mechanism in the sample with the composition $VS_{1.60}$. As mentioned above, the sample shows a series of transitions; V_5S_8 type → V_3S_4 type → CdI_2 type. It is to be noted that the metal sites in the partially filled layer of the V_3S_4-type structure with the composition $VS_{1.60}$ are partially occupied (50%) instead of being perfectly occupied (100%) for the composition $VS_{1.33}$ (stoichiometric V_3S_4). Now let us consider the process of phase transition from the V_5S_8- to the V_3S_4-type structure for the case of the composition $VS_{1.60}$. At first glance, the disordering along the *a* or *b* axis of the V_5S_8-type structure (an array of alternate arrangement of metal and vacancy) leads to the V_3S_4-type structure. In this case, the following relations must hold (see Fig. 9a):

$$\mathbf{a}(V_3S_4) = \tfrac{1}{2}\mathbf{a}(V_5S_8), \qquad \mathbf{b}(V_3S_4) = \tfrac{1}{2}\mathbf{b}(V_5S_8),$$
$$\mathbf{c}(V_3S_4) = \tfrac{1}{2}\mathbf{c}(V_5S_8). \tag{1}$$

This mechanism is at variance with the experimental results as follows.

(i) The lattice parameter $c(V_3S_4)$ is nearly equal to that of $c(V_5S_8)$ as shown in Fig. 8.

(ii) The temperature dependence of the lattice spacing along the *a* and *b* axis shows marked discontinuity at T_{c_2} as shown in Fig. 10. This conflicts with the fact that the phase transition at T_{c_2} is of second order.

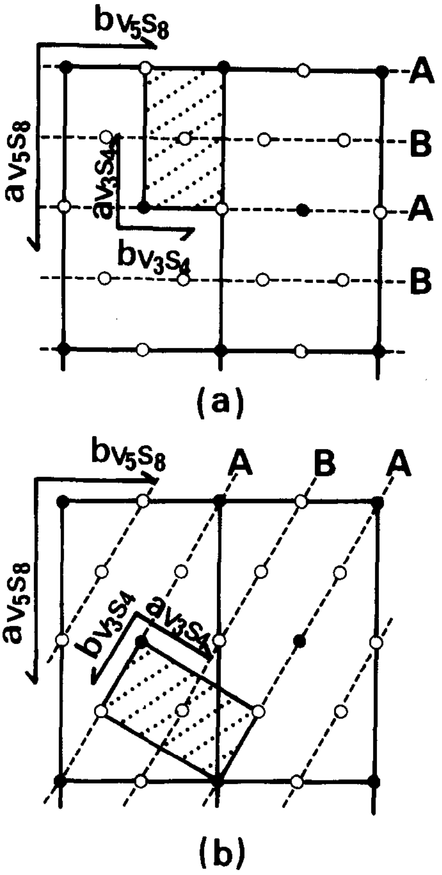

FIG. 9. Schematic illustration of the metal and vacancy arrangement in the partially filled layer with the composition $VS_{1.60}$. Filled circles indicate the vanadium atoms and open circles indicate the vacancy sites. a and b are the unit cell vectors for the V_5S_8 type and the V_3S_4 type. (a) and (b) show the possible mechanism for the transition from the V_5S_8 type to the V_3S_4 type (see text).

Figure 9b shows another possibility for the mechanism of the phase transition. The partially filled layer of the V_5S_8-type structure can be regarded as the alternate arrangement of chains A and B. Chain A consists of alternate metal and vacancy sites, and chain B of only vacancy sites. The intra-chain disordering in chain A again leads to the V_3S_4-type structure of which the unit cell is shown in Fig. 8. In this case the following relations must hold:

$$\begin{aligned}\mathbf{a}(V_3S_4) &= \tfrac{1}{4}\{\mathbf{a}(V_5S_8) + 3\mathbf{b}(V_5S_8)\},\\ \mathbf{b}(V_3S_4) &= \tfrac{1}{4}(\mathbf{a}(V_5S_8) + \mathbf{b}(V_5S_8)\},\\ \mathbf{c}(V_3S_4) &= \mathbf{c}(V_5S_8).\end{aligned} \qquad (2)$$

With this model, the temperature dependence of the lattice spacings corresponding to the *a* and *b* axis of the hypothetical V_5S_8-type structure above T_{c_2} were recalculated up to 910°C. As shown in Fig. 10, the lattice spacings smoothly increase with increasing temperature through T_{c_2}. In Fig. 10 the temperature dependence of the unit-cell volume which smoothly connects at T_{c_2} is also shown. It supports the suggestion that the transition may be of second order. This is quite consistent with the experimental facts.

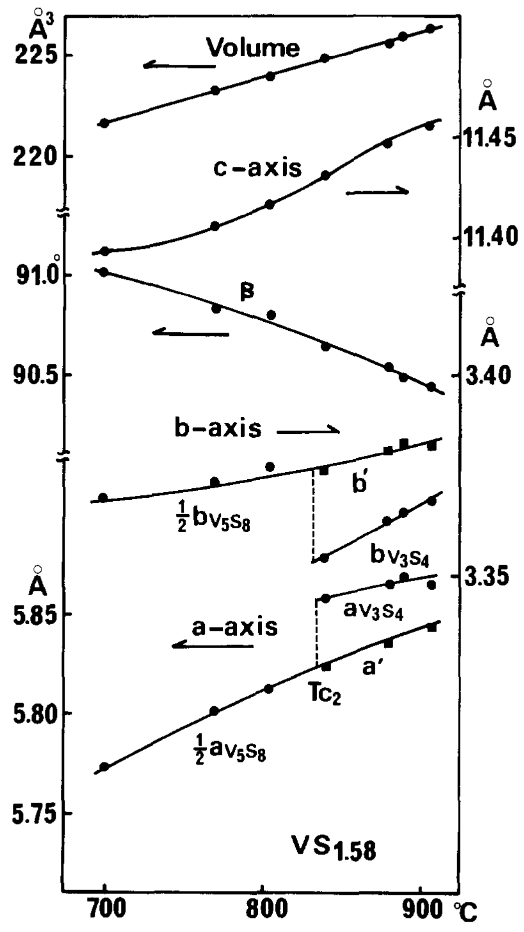

FIG. 10. The lattice parameters and the unit-cell volume vs temperature curves for the sample with the composition $VS_{1.58}$. Closed circles are the measured values and closed squares are the calculated values by Eq. (2) from the measured values.

Thus it can be concluded that the origin of the phase transition from the V_5S_8- to the V_3S_4-type structure is intra-chain disordering. The phase transition from the V_3S_4- to the CdI_2-type structure can be regarded as the result of inter-chain disordering within the same plane, or intralayer disordering. At higher temperature, the interlayer disordering between partially filled metal layers and perfectly filled metal layers should take place and this mechanism corresponds to a transition from the CdI_2- to the NiAs-type structure. However, in the present work up to 1200°C, this transition has not been observed. It should occur at a considerably higher temperature.

As for the statistical thermodynamic treatment of the order–disorder transition for these systems, we will discuss it in a following paper which will appear in the near future (*10*).

Acknowledgments

The authors are grateful to Professor M. Koizumi and Dr. M. Shimada for the use of the high-temperature DTA apparatus. Thanks are also due to Professor T. Sato and Professor O. Uemura for the experiment on the high-temperature X-ray camera, and to Dr. H. Asano for the specific heat measurement.

References

1. G. A. WIEGERS AND F. JELLINEK, *J. Solid State Chem.* **1**, 519 (1970).
2. Y. OKA, K. KOSUGE, AND S. KACHI, *Phys. Lett. A* **50**, 311 (1974).
3. A. B. DE VRIES AND F. JELLINEK, *Rev. Chim. Miner.* **11**, 624 (1974).
4. F. JELLINEK, *Acta Crystallogr.* **10**, 620 (1957).
5. F. GRØNVOLD, *Acta Chem. Scand. 22*, 1219 (1968). S. MURANAKA, *Mater. Res. Bull.* **8**, 679 (1973).
6. H. NAKAZAWA, M. SAEKI, AND M. NAKAHIRA, *J. Less Common Metals* **40**, 57 (1975).

7. M. Chevreton and A. Sapet, *C.R. Acad. Sci., Paris* **261**, 928 (1965).
8. S. Brunie and M. Chevreton, *C.R. Acad. Sci., Paris* **258**, 5847 (1964).
9. I. Kawada, M. Nakano-Onoda, M. Ishii, and M. Nakahira, *J. Solid State Chem.* **15**, 246 (1975).
10. Y. Oka, K. Kosuge, and S. Kachi, *J. Solid State Chem.*, in press.